Clinical & Translational Immunology

Australian and New Zealand Society for Immunology Inc.

Clinical & Translational Immunology 2021; e1357. doi: 10.1002/cti2.1357
www.wileyonlinelibrary.com/journal/cti

SHORT COMMUNICATION

Blunted sFasL signalling exacerbates TNF-driven neutrophil necroptosis in critically ill COVID-19 patients

Tiziano A Schweizer[1†], Srikanth Mairpady Shambat[1†], Clement Vulin[1], Sylvia Hoeller[2], Claudio Acevedo[1], Markus Huemer[1], Alejandro Gomez-Mejia[1], Chun-Chi Chang[1], Jeruscha Baum[1], Sanne Hertegonne[1], Eva Hitz[1], Thomas C Scheier[1], Daniel A Hofmaenner[3], Philipp K Buehler[3], Holger Moch[2], Reto A Schuepbach[3], Silvio D Brugger[1] & Annelies S Zinkernagel[1]

[1]Department of Infectious Diseases and Hospital Epidemiology, University Hospital of Zurich, University of Zurich, Zurich, Switzerland
[2]Department of Pathology and Molecular Pathology, University Hospital of Zurich, University of Zurich, Zurich, Switzerland
[3]Institute for Intensive Care Medicine, University Hospital of Zurich, University of Zurich, Zurich, Switzerland

Correspondence
AS Zinkernagel, Department of Infectious Diseases and Hospital Epidemiology, University Hospital of Zurich, Rämistrasse 100, Zurich 8091, Switzerland.
Email: annelies.zinkernagel@usz.ch

[†]Equal contributors.

Received 22 June 2021;
Revised 26 October 2021;
Accepted 3 November 2021

doi: 10.1002/cti2.1357

Clinical & Translational Immunology
2021; **10**: e1357

Abstract

Objectives. Critically ill coronavirus disease 2019 (COVID-19) patients are characterised by a severely dysregulated cytokine profile and elevated neutrophil counts, impacting disease severity. However, it remains unclear how neutrophils contribute to pathophysiology during COVID-19. Here, we assessed the impact of the dysregulated cytokine profile on the regulated cell death (RCD) programme of neutrophils. **Methods.** Regulated cell death phenotype of neutrophils isolated from critically ill COVID-19 patients or healthy donors and stimulated with COVID-19 or healthy plasma *ex vivo* was assessed by flow cytometry, time-lapse microscopy and cytokine multiplex analysis. Immunohistochemistry of COVID-19 patients and control biopsies were performed to assess the *in situ* neutrophil RCD phenotype. Plasma cytokine levels of COVID-19 patients and healthy donors were measured by multiplex analysis. Clinical parameters were correlated to cytokine levels of COVID-19 patients. **Results.** COVID-19 plasma induced a necroptosis-sensitive neutrophil phenotype, characterised by cell lysis, elevated release of damage-associated molecular patterns (DAMPs), increased receptor-interacting serine/threonine-protein kinase (RIPK) 1 levels and mixed lineage kinase domain-like pseudokinase (MLKL) involvement. The occurrence of neutrophil necroptosis MLKL axis was further confirmed in COVID-19 thrombus and lung biopsies. Necroptosis was induced by the tumor necrosis factor receptor 1 (TNFRI)/TNF-α axis. Moreover, reduction of soluble Fas ligand (sFasL) levels in COVID-19 patients and hence decreased signalling to Fas directly increased RIPK1 levels, exacerbated TNF-driven necroptosis and correlated with disease severity, which was abolished in patients treated with glucocorticoids. **Conclusion.** Our results suggest a novel role for sFasL signalling in the TNF-α-induced RCD programme in neutrophils during COVID-19 and a potential therapeutic target to curb inflammation and thus influence disease severity and outcome.

Keywords: COVID-19, Fas (CD95), necroptosis, neutrophils, RIPK1, TNF-α

INTRODUCTION

Patients experiencing severe COVID-19, caused by SARS-CoV-2, are at risk for respiratory failure and elevated mortality.[1] The current state of knowledge indicates a strongly dysregulated immune response during critical COVID-19, affecting the phenotype of various cells, including neutrophils.[2] Neutrophils might contribute to immunothrombosis and lung injury in critical COVID-19 patients because of increased NETs, as indicated by the presence of extracellular DNA colocalised with myeloperoxidase (MPO), citrullinated histones or elastase in tracheal aspirates and histological lung sections.[3,4] However, intracellular content might also be released during necroptosis.[5] Necroptosis is initiated by ripoptosome assembly, which can either induce apoptosis and necroptosis or promote cell survival, depending on its stoichiometric composition of the key components RIPK1, caspase-8, Fas-associated protein with death domain (FADD) and cellular FADD-like IL-1β-converting enzyme inhibitory protein (cFLIP) isoforms.[6] In case of stabilised RIPK1 and availability of downstream effector proteins,[7] necroptosis is driven by RIPK1-RIPK3 necrosome formation and subsequent MLKL activation, inducing cell rupture.[8] Assembly and functionality of the ripoptosome is strictly regulated, among others, by the TNFRI/TNF-α or Fas/FasL system.[9] However, whether skewed RCD mechanisms of neutrophils contribute towards augmenting tissue injury and inflammation in COVID-19 remains unclear. Importantly, given that neutrophil counts are significantly elevated in critically ill COVID-19 patients, necroptosis could possibly contribute to severe inflammation in these patients.

Here, we report a TNF-α-induced necroptosis-sensitive neutrophil subpopulation in critically ill COVID-19 patients, because of increased RIPK1-dominant function and execution of necroptosis through RIPK3-MLKL, augmented by impaired Fas/sFasL signalling, which correlated with disease severity.

RESULTS

Neutrophils were isolated from critically ill COVID-19 patients enrolled in our prospective intensive care unit (ICU) cohort (Supplementary tables 1 and 2) within the first 4 days upon ICU admission ($n = 61$). In parallel, neutrophils from healthy donors were isolated. COVID-19 or healthy donor neutrophils stimulated with autologous or heterologous plasma were assessed for short-term viability by flow cytometry (Figure 1a, Supplementary figure 1a–c). Stimulation with acute-phase COVID-19 plasma decreased the proportion of live cells and increased the proportion of RCD of COVID-19 and healthy donor neutrophils in 8 of 10 cases (Figure 1b and c). No differences in neutrophil viability were observed when the same patients were assessed in their recovery-phase (Figure 1d), highlighting a transient effect of acute-phase COVID-19 plasma on RCD induction.

Time-lapse microscopy of neutrophils, using the cell-permeable DNA-dye Hoechst and the cell-impermeable DNA-dye SYTOX™ Green, revealed a lytic RCD form, linked to expulsion of DNA in COVID-19 neutrophils, but distinct from classical NET formation (Figure 1e, Supplementary figure 2a, b, Supplementary videos 1, 2).[10] When assessing cell death kinetics, COVID-19 neutrophils died at a higher rate (becoming SYTOX+) when stimulated with autologous plasma as compared to heterologous plasma, resulting in a significantly increased proportion of dead cells (Figure 1f–h, Supplementary figure 3a–c). The sensitivity of our time-lapse microscopy was further verified by using neutrophils from a COVID-19 patient concomitantly treated with tamoxifen, known to promote NET formation,[11] in which classical NETs (Supplementary figure 2c, d) and apoptotic bodies were observed (Supplementary figure 2e, f).

Pan-caspase-, caspase-1- or caspase-8-specific inhibition showed no effect on short-term survival of neutrophils stimulated with COVID-19 plasma (Supplementary figure 4a, b), confirming that neutrophils underwent caspase-independent lytic RCD (Figure 2a and b). When assessing long-term survival, COVID-19 plasma stimulation had the opposite outcome as compared to short-term stimulation, with higher proportions of neutrophils surviving as compared to healthy plasma stimulation (Figure 2c and d). Caspase inhibition significantly elevated the proportion of long-term surviving neutrophils, but to a

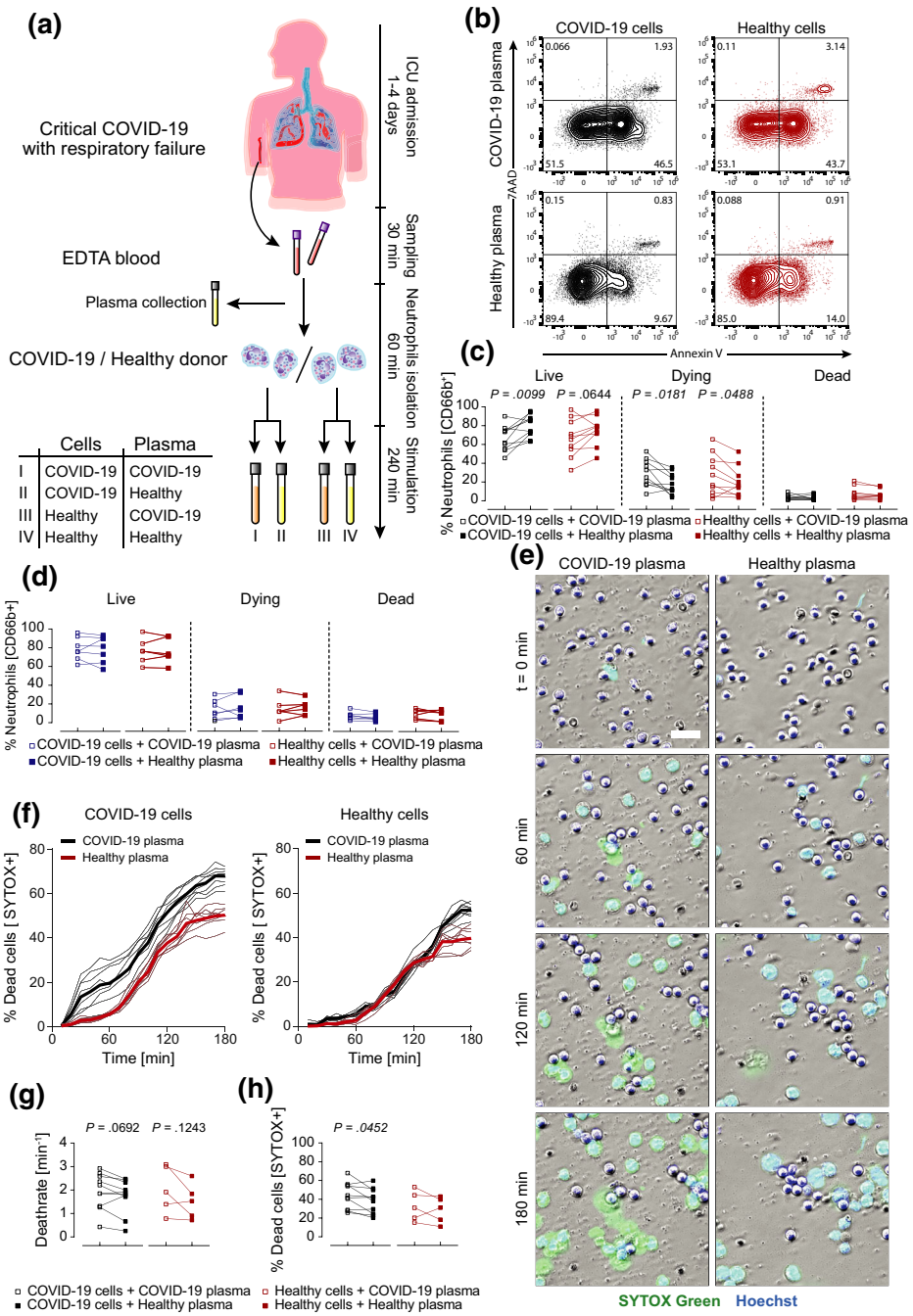

Figure 1. COVID-19 acute-phase plasma induces lytic regulated cell death (RCD) of neutrophils. **(a)** Experimental overview. **(b, c)** Representative flow cytometry plot of one experiment from acute-phase COVID-19 ($n = 10$) and healthy donor ($n = 10$) neutrophils stimulated with autologous or heterologous plasma for 4 h, **(b)** and quantification of live (Annexin $V^-/7AAD^-$), dying (Annexin $V^+/7AAD^-$) and dead (Annexin $V^+/7AAD^+$) neutrophils **(c)**. **(d)** Quantification of live, dying and dead recovery-phase COVID-19 ($n = 7$) or healthy donor ($n = 6$) neutrophils stimulated with autologous or heterologous plasma for 4 h. **(e)** Representative time-lapse microscopy of acute-phase COVID-19 neutrophils stimulated with autologous or heterologous plasma for 3 h. Cells were stained with Hoechst 33342 (blue) and SYTOX™ Green. Images were taken every 10 min. Scale bar, 30 µm. **(f)** Representative cell death curve. Thin lines are FOV ($n = 8$) per condition, and thick line is the mean of FOVs. Left: COVID-19 neutrophils; right: healthy neutrophils. **(g, h)** Quantification of cell death rate **(g)** and proportion **(h)** at 3 h of COVID-19 ($n = 10$) or healthy neutrophils ($n = 5$) stimulated with autologous or heterologous plasma. See also Supplementary videos 1, 2. Connected squares represent one donor. Statistics were calculated by the paired *t*-test or Wilcoxon signed-rank test. *P*-values are indicated within the graphs. FOV, field of view.

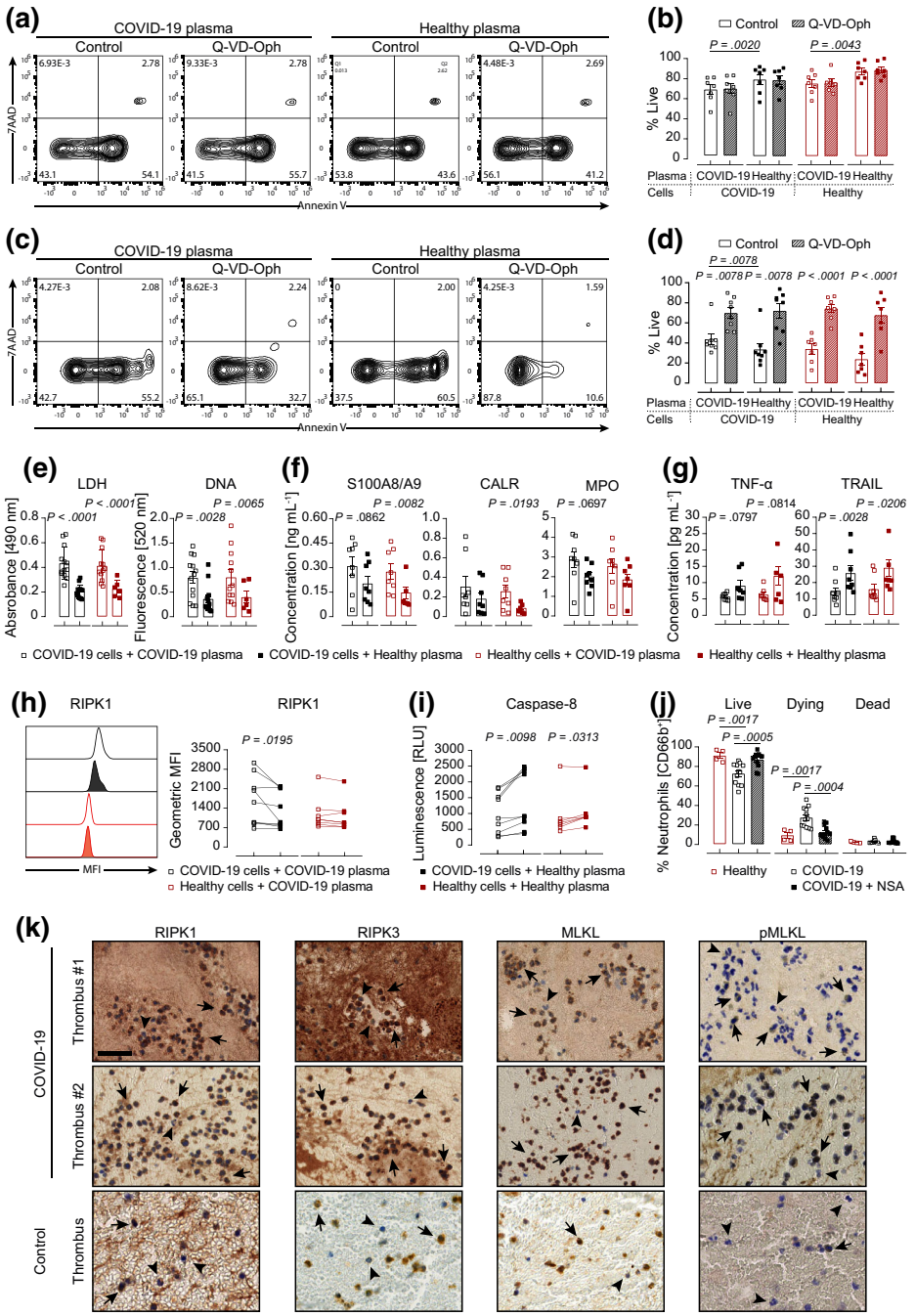

Figure 2. Neutrophil necroptosis through the RIPK1-RIPK3-MLKL axis in COVID-19. **(a–d)** Representative flow cytometry plots at 4 h **(a)** or 18 h post-stimulation, **(c)** and quantification of live COVID-19 ($n = 7$ or 8) or healthy donor ($n = 7$) neutrophils stimulated with autologous or heterologous plasma, untreated or treated with 50 μM Q-VD-Oph for 4 h **(b)** or 18 h **(d)**. **(e–g)** Analysis of LDH and DNA, **(e)** and DAMPs **(f)** and cytokines **(g)** in supernatants of COVID-19 ($n = 7$ or 13) or healthy donor ($n = 6$ or 7) neutrophils stimulated with autologous or heterologous plasma for 4 h. **(h, i)** Representative histogram and quantification of GMFI of intracellular RIPK1 expression **(h)** and caspase-8 activity **(i)** of COVID-19 ($n = 9$) or healthy donor ($n = 6$ or 7) neutrophils stimulated with autologous or heterologous plasma for 4 h. **(j)** Quantification of live (Annexin V^-/7AAD$^-$), dying (Annexin V^+/7AAD$^-$) and dead (Annexin V^+/7AAD$^+$) healthy donor neutrophils ($n = 4$) stimulated with healthy or COVID-19 plasma ($n = 12$), untreated or treated with 5 μM NSA for 4 h. For each experiment, healthy donor neutrophils were stimulated separately with plasma from three different COVID-19 patients. Each square or connected squares represent one donor. Shown are mean ± SEM. Statistics were calculated by the paired *t*-test or the Wilcoxon signed-rank test. *P*-values are indicated within the graphs. **(k)** RIPK1, RIPK3, MLKL and pMLKL staining of COVID-19 ($n = 2$) and non-COVID-19 thrombi. Scale bar, 50 μm. Arrows indicate strong positive staining, and arrowheads indicate negative or weak positive staining. NSA, necrosulphonamide; SEM, standard error of means.

lesser extent in the COVID-19 environment (Supplementary figure 4c), proposing a caspase-impaired environment, favoring the occurrence of a necroptosis-sensitive subpopulation. We assessed the release of selected DAMPs and classical cytokines, such as members of the TNF superfamily, as a proxy for neutrophil necroptosis. COVID-19 plasma stimulation resulted in significantly higher lactate dehydrogenase (LDH), DNA, S100A8/A9 and calreticulin (CALR) as well as slightly elevated MPO release as compared to healthy plasma stimulation (Figure 2e and f) and decreased levels of TNF-α and TRAIL (Figure 2g). Furthermore, we also assessed intracellular RIPK1 levels and caspase-8 activity. Neutrophils from COVID-19 patients stimulated with autologous plasma displayed significantly higher RIPK1 levels (Figure 2h) and decreased caspase-8 activity (Figure 2i) as compared to healthy plasma stimulation in 8 of 9 and 9 of 9 cases, respectively. This observed phenotype was similarly identified upon necroptosis induction in healthy neutrophils (Supplementary figure 5). Finally, MLKL inhibition rescued COVID-19 plasma-induced RCD, confirming the occurrence of necroptosis (Figure 2j). Histological analysis within thrombus biopsies of COVID-19 patients (Supplementary table 3) showed strong positive staining for the necroptosis markers RIPK1, RIPK3, MLKL and phosphorylated MLKL (pMLKL) for neutrophils (Figure 2k, Supplementary figure 6), corroborating the observed necroptosis-sensitive neutrophil phenotype. We also observed evidence for neutrophil necroptosis in a thrombus from a non-COVID-19 patient suffering from an aneurysm, but to a lesser extent with lower neutrophil numbers as compared to COVID-19 thrombi (Figure 2k). Furthermore, we discovered strong positive staining of necroptosis markers in COVID-19 lung biopsy tissue (Supplementary figure 6a), especially neutrophils, which were always strongly stained within blood vessels (Supplementary figure 6b).

We previously detected significantly elevated TNF-α levels in our COVID-19 ICU cohort,[12] known to modulate RCD. However, the expression of the TNFRI receptor on neutrophils from COVID-19 patients showed only a tendency towards decreased expression as compared to healthy donors (Figure 3a). Nevertheless, blocking TNFRI of healthy donor neutrophils stimulated with COVID-19 plasma resulted in significantly elevated viability as compared to no blocking (Figure 3b), while blocking of TNFRII showed no effect (Supplementary figure 7a). Furthermore, the addition of exogenous TNF-α to COVID-19 plasma stimulation led to enhanced necroptosis in healthy donor neutrophils, which was reverted by MLKL inhibition (Figure 3c). Interestingly, when looking at two other well-known death receptor pathways, which gained attention in COVID-19, we observed significantly lower sFasL concentrations in plasma from COVID-19 patients as compared to healthy donors, and equal levels of TRAIL (Figure 3d). During the recovery phase of these patients, the concentration of sFasL normalised, reaching same levels as of healthy donors (Supplementary figure 7b). Assessing the corresponding receptors, we observed significantly higher Fas expression on neutrophils from COVID-19 patients as compared to healthy donors, whereas TRAIL-R1 expression displayed no difference (Figure 3e). Interestingly, the supernatant of COVID-19 neutrophils contained significantly lower sFasL concentrations when stimulated with autologous plasma as compared to heterologous plasma (Figure 3f), which was linked to decreased intracellular production of FasL (Figure 3g), but no changes in membrane-bound FasL (mFasL) were observed (Supplementary figure 7c).

The addition of recombinant sFasL to COVID-19 neutrophils significantly decreased RCD induction in the COVID-19 environment (Figure 3h and i). Blocking sFasL binding to Fas by a Fas-blocking antibody, however, increased the rate of RCD significantly, also during healthy plasma stimulation (Figure 3j and k). Additionally, Fas blocking upon TNF-α-induced necroptosis in healthy donor neutrophils enhanced RCD, which was completely reverted by MLKL inhibition (Supplementary figure 7e), while Fas blocking without RCD stimulus did not affect viability (Supplementary figure 7f). Furthermore, we found that treatment with sFasL decreased RIPK1 levels significantly during COVID-19, but not healthy, plasma stimulation (Figure 3l), independent of caspase-8 (Figure 3m) and caspase-3/7 (Figure 3n) activity.

When evaluating key COVID-19 severity markers, neutrophil-to-lymphocyte ratio (NLR), monocytes, IL-6, CRP, bilirubin, platelets, length of ventilation (LOV) and length of ICU stay (LOS)[13,14] with sFasL levels, no significant correlation was observed (Supplementary figure 8a). However, in-depth analysis of patients treated either by attending physicians' discretion standard of care (USZ SOC) or according to the guidelines of the RECOVERY

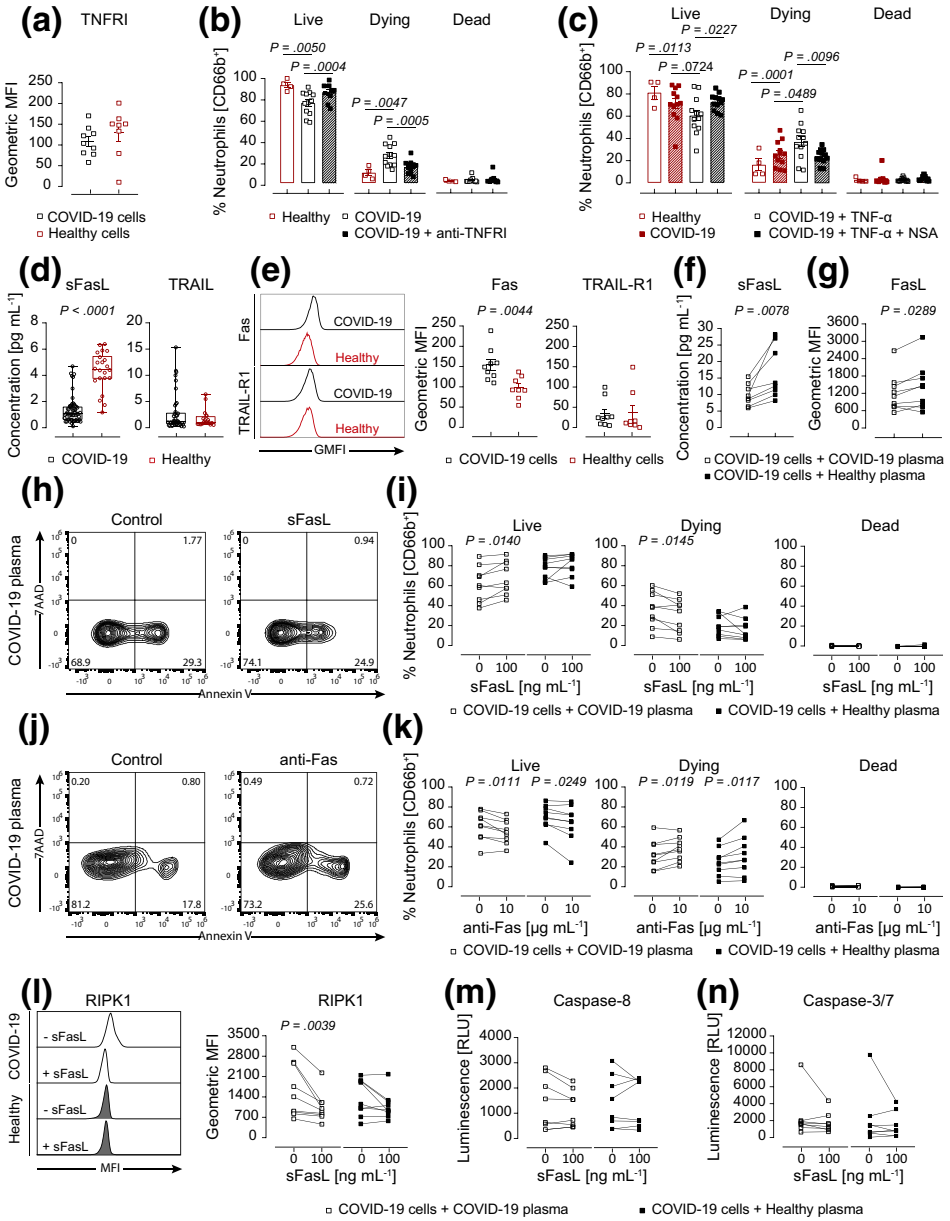

Figure 3. Impaired sFasL signalling during COVID-19 favors RIPK1-driven necroptosis. **(a)** TNFRI expression on COVID-19 ($n = 9$) and healthy donor neutrophils ($n = 8$). **(b, c)** Quantification of live (Annexin V^-/$7AAD^-$), dying (Annexin V^+/$7AAD^-$) and dead (Annexin V^+/$7AAD^+$) healthy donor neutrophils ($n = 4$) stimulated with healthy or COVID-19 plasma ($n = 12$), untreated or treated with 2 μg mL^{-1} anti-TNFRI **(b)** or with 30 ng mL^{-1} TNF-α with or without 5 μM NSA **(c)**. For each experiment, healthy donor neutrophils were stimulated separately with plasma from three different COVID-19 patients. **(d)** Luminex-based analysis of COVID-19 (sFasL, $n = 56/61$; TRAIL, $n = 28/61$ detected) and healthy donors' plasma (sFasL, $n = 22/22$; TRAIL, $n = 17/22$). **(e)** Representative histogram and quantification of receptor expression on neutrophils from COVID-19 ($n = 9$) and healthy donors ($n = 8$). **(f, g)** Luminex-based analysis of sFasL in supernatants **(f)** and quantification of intracellular FasL expression **(g)** of COVID-19 neutrophils ($n = 8$ or 9) stimulated with autologous or heterologous plasma for 4 h. **(h, i)** Representative flow cytometry plots **(h)** and quantification of live, dying and dead **(i)** COVID-19 neutrophils ($n = 9$) stimulated with autologous or heterologous plasma and with or without 100 ng mL^{-1} sFasL for 4 h. **(j, k)** Representative flow cytometry plots **(j)** and quantification of live, dying and dead **(k)** COVID-19 neutrophils ($n = 9$) stimulated with autologous or heterologous plasma and with or without 10 μg mL^{-1} anti-Fas for 4 h. **(l–n)** Representative histogram and quantification of GMFI of intracellular RIPK1 expression **(l)**, caspase-8 activity **(m)** or caspase-3/7 activity **(n)** of COVID-19 neutrophils ($n = 8$ or 9) stimulated with autologous or heterologous plasma and with or without 100 ng mL^{-1} sFasL for 4 h. Each dot, each square or connected squares represent one donor. Shown are mean ± SEM. Statistics were calculated by the unpaired *t*-test, Mann–Whitney *U*-test, paired *t*-test or Wilcoxon signed-rank test. *P*-values are indicated within the graphs. NSA, necrosulphonamide; SEM, standard error of means.

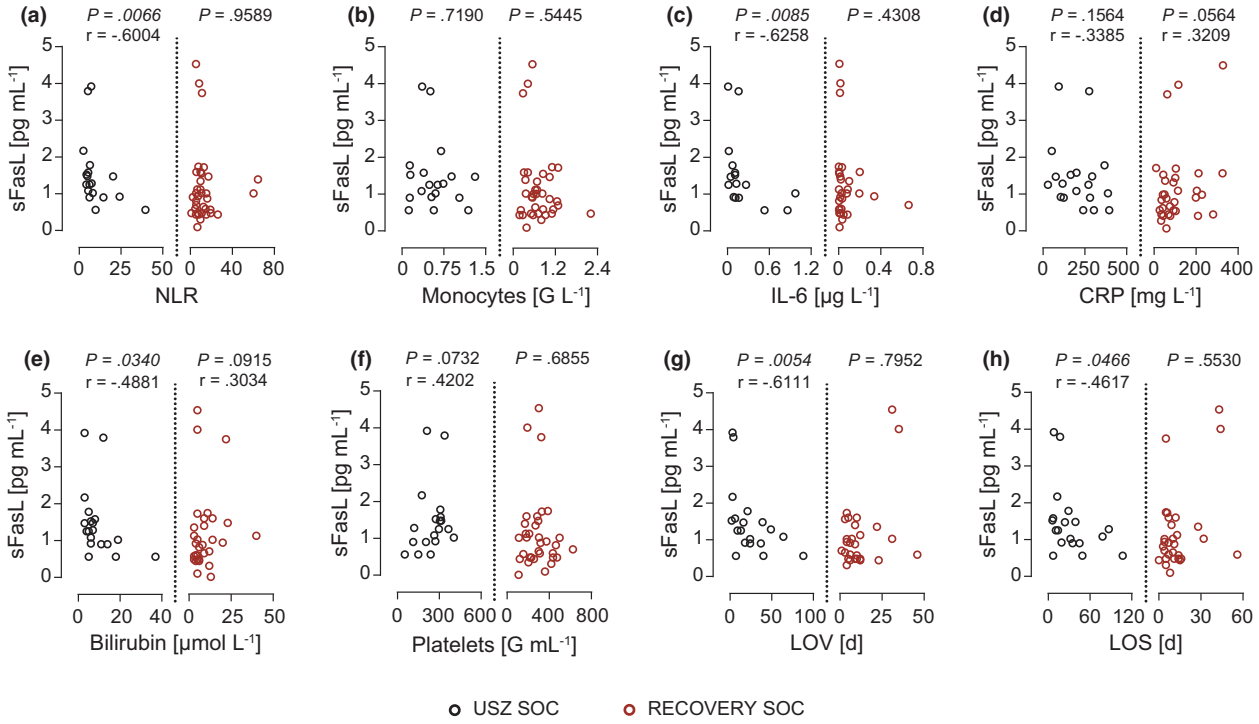

Figure 4. Correlation of low sFasL levels with disease severity in COVID-19 patients and abolishment by RECOVERY SOC. **(a–h)** Correlation analysis of plasma sFasL levels with NLR **(a)**, monocytes **(b)**, IL-6 **(c)**, CRP **(d)**, bilirubin **(e)**, platelets **(f)**, LOV **(g)** and LOS **(h)** in the USZ ($n = 19$) and RECOVERY SOC ($n = 36$) group. Each dot represents one donor for which sFasL was detected ($n = 55$). One patient from the RECOVERY SOC group received dexamethasone only after experimental sampling and was excluded from the correlation analysis. Statistics were calculated by the non-parametric Spearman correlation. NLR, neutrophil-to-lymphocyte ratio; LOV, length of ventilation; LOS, length of ICU stay; USZ, University Hospital Zurich; SOC, standard of care.

trial (RECOVERY SOC),[15] that is dexamethasone, a significant negative correlation between sFasL levels and NLR and IL-6, but not monocytes or CRP (Figure 4a–d), was observed in the USZ SOC group. Low sFasL levels also correlated with high bilirubin, low platelets, and increased LOV and LOS (Figure 4e–h). No correlation of sFasL with disease severity was observed in the RECOVERY SOC, even though sFasL levels were similar in both groups (Supplementary figure 8b). Furthermore, neutrophils from COVID-19 patients treated under RECOVERY SOC showed enhanced viability compared with USZ SOC (Supplementary figure 8c), which was in line with significantly lower TNF-α plasma levels in RECOVERY SOC as compared to USZ SOC patients (Supplementary figure 8d).

DISCUSSION

We found that neutrophils from critically ill COVID-19 patients frequently succumbed to rapid lytic RCD. Healthy donor neutrophils stimulated with plasma from critically ill COVID-19 patients also exhibited a similar rapid lytic RCD. This observation was in accordance with findings by Middleton *et al.*, reported as NETs.[3] However, we recently showed that neutrophils from COVID-19 patients released significantly fewer classical NETs upon secondary bacterial challenge.[12] Rapid lytic RCD in a subpopulation, but increased long-term survival of neutrophils in the COVID-19 environment, might be explained by elevated levels of certain cytokines, such as G-CSF, GM-CSF and IL-8 during COVID-19,[2,12] known to interfere with caspase activation. Additionally, certain viruses are known to produce caspase-8-interfering peptides[16]; whether these are produced by SARS-CoV-2 is yet to be identified. Importantly, in case of caspase impairment, blocking of necroptosis is required to ensure prolonged survival.[9] Previous studies have shown that elevated RIPK1 mRNA expression or protein levels are reliable markers for necroptosis detection.[17] Therefore, increased RIPK1 levels, elevated DAMP release and confirmation of MLKL involvement in the COVID-19 environment

suggested a necroptosis-sensitive neutrophil subpopulation. DAMPs, especially S100A8/A9, have previously been described to be important drivers of COVID-19 pathogenesis.[18] Together with our histological findings, this might suggest that neutrophil necroptosis and the release of intracellular content favor the formation of endothelial damage and thrombi during COVID-19.[3,19] However, further research is warranted to determine whether neutrophil necroptosis activates platelets or vice versa.[5] The findings of neutrophil necroptosis in COVID-19 thrombi or lungs are in line with studies showing that intracellular neutrophil content in tissue can originate from RIPK1-RIPK3-MLKL-mediated necroptosis,[20] and therefore seems to be not unique for COVID-19.

TNFRI/TNF-α axis involvement in the observed necroptotic phenotype is not surprising, since this is the most well-known mediator of necroptosis.[21] However, low sFasL levels exacerbated necroptosis unexpectedly. The Fas/FasL axis has recently gained attention in COVID-19, with decreased plasma sFasL levels,[22] as also observed in our cohort. The signalling modality of FasL to Fas not only during inflammation but also under homeostasis is still not completely understood. In general, deducted from T-cell research, FasL can occur as sFasL, acting as a pro-survival signal, whereas mFasL induces RCD.[8,23] For neutrophils, it was also shown that mFasL induces cell death, whereas sFasL is known to drive activation and chemotaxis.[24–26] In line with our findings of increased Fas expression on neutrophils, suggesting decreased receptor engagement, a similar increased Fas expression on T cells during COVID-19 was recently reported.[27] Therefore, our findings propose that sFasL acts as a pro-survival signal for neutrophils upon TNF-α-mediated necroptosis, with its expression and secretion being altered during COVID-19.

The observed correlation of sFasL with increased IL-6 and NLR might suggest that neutrophil necroptosis because of decreased sFasL levels favors an inflammation feedback loop with a central role for IL-6 signalling,[28] potentially sustaining emergency granulopoiesis and aborting lymphopoiesis.[29] However, it needs to be clarified how decreased sFasL levels affect lymphocyte viability. Nevertheless, the correlation analysis with platelets and bilirubin further highlighted the devastating effect of neutrophil necroptosis on coagulation and tissue damage, shown to impact COVID-19 severity.[4,30] Previously, decreased sFasL levels have been linked to increased mortality in burn patients[31] and increased disease activity in Sjogren's syndrome,[32] thereby corroborating our findings that sFasL might play an important role in protection from tissue damage in COVID-19.

The publication of the RECOVERY trial data led to standard usage of dexamethasone in most critically ill COVID-19 patients.[14] Synthetic glucocorticoids favor neutrophil maturation, survival and tissue retention.[33] The absence of correlations of sFasL in the RECOVERY SOC group might be explained by the fact that glucocorticoid treatment potentially ameliorated disease severity by either accelerating neutrophil maturation or dampening the inflammatory COVID-19 environment, leaving neutrophils less sensitive to necroptosis. However, prescription of synthetic glucocorticoids during viral pneumonia is still controversial, as the timing, dosage and duration of application play an important role in defining the potential beneficial or detrimental effect on outcome.[34] Therefore, directly targeting the effectors involved in the necroptosis axis might offer a valid alternative, aiming to improve inflammation resolution.

Although the findings presented in this work were obtained from a small cohort at a single centre, they nevertheless further elucidate the crucial role of neutrophils during COVID-19 and deliver novel insights into the role of the Fas/FasL system upon TNF-α-induced necroptosis in neutrophils, and its correlation with disease severity. These results suggest a previously unrecognised, albeit small, role for sFasL in promoting neutrophil survival in an inflammatory TNF-α prominent context. Our findings provide hints for future potential therapeutic development, aiming at restoring the fate of neutrophils and benefiting patient outcome, potentially beyond COVID-19.

METHODS

Patients and healthy donors

Patients were recruited between April and December 2020 in the MicrobiotaCOVID prospective cohort study conducted at the Institute of Intensive Care Medicine of the University Hospital Zurich (USZ, Zurich, Switzerland) and were included in an extended subcohort as described previously.[12,35] The study was approved by the local ethics

committee of the Canton of Zurich, Switzerland (Kantonale Ethikkommission Zurich BASEC ID 2020 – 00646), and is registered at clinicaltrials.gov (ClinicalTrials.gov Identifier: NCT04410263). Patients were considered to be in the acute-phase within the first four days upon initial ICU admission, and the recovery-phase was defined as patients being discharged from the ICU or negative for SARS-CoV-2 and in a non-critical state. Blood sampling was carried out with EDTA tubes. Patient demographics and clinical and laboratory parameters are listed in Supplementary table 1. Blood sampling for isolation of neutrophils and plasma collection from healthy volunteers was approved by the local ethics committee of the Canton of Zurich, Switzerland (Kantonale Ethikkommission Zurich BASEC ID 2019 – 01735).

Plasma collection

EDTA tubes were centrifuged at 700 *g* for 10 min (no acceleration and brakes) after which the plasma was separated from the cellular fraction and collected in a fresh tube. The cellular fraction of the blood was used for neutrophil isolation as described below. The collected plasma was centrifuged again at 1900 *g* for 10 min (full acceleration and brakes) to pellet debris, and the clear plasma supernatant was collected. Plasma samples were either used directly for the experiments or aliquoted and frozen at −80°C for cytokine analysis.

Cytokine analysis

Cytokine levels in plasma from COVID-19 patients and healthy donors, as well as cell culture supernatants, were analysed on a Luminex™ MAGPIX™ instrument with a custom human cytokine panel (Thermo Fisher, Waltham MA, USA). Samples were thawed at room temperature and prepared according to the manufacturer's instructions. In brief, magnetic beads were added to the 96-well plate on a magnetic holder and incubated for 2 min. The plate was washed twice with assay buffer for 30 s each. Provided standards were diluted in assay buffer or RPMI (Gibco, Thermo Fisher) for analysis of plasma levels or cell culture supernatants. Cell culture supernatants were measured undiluted, whereas plasma samples were diluted 1:2 in assay buffer. The plate was incubated for 2 h at room temperature (RT) at 550 rpm in an orbital plate shaker. Next, the plate was washed twice and incubated for 30 min at 550 rpm with detection antibodies. Following further washing steps, the plate was incubated with Streptavidin-PE solution for 30 min at 550 rpm. Finally, the plate was washed, and reading buffer was added and incubated for 10 min at RT and 550 rpm before running the plate. Analysis was performed using the xPONENT® software. Data were validated additionally with the ProcartaPlex Analyst software (Thermo Fisher).

Isolation of neutrophils and plasma stimulation

Neutrophils from COVID-19 patients and healthy donors were isolated with the EasySep™ Direct Human Neutrophil Isolation Kit (StemCell™, Vancouver, CA) according to the manufacturer's instructions. In brief, the cellular fraction of the blood was diluted 1:2 with Dulbecco's phosphate-buffered saline (DPBS, Gibco) and neutrophil enrichment cocktail was added for 15 min. Next, the magnetic beads were added for 15 min. The samples were once more diluted 1:2 with DPBS and placed in a magnetic holder (StemCell™) for 15 min. Neutrophils were collected and centrifuged for 500 *g* (low acceleration and brakes) for 5 min. Red blood cell lysis was performed with H_2O and stopped with DPBS after which the samples were centrifuged. Neutrophils were resuspended in RPMI and counted on an Attune NxT (Thermo Fisher). Neutrophils were either directly stained for cell surface receptor analysis using flow cytometry or prepared in RPMI containing 10% either autologous or heterologous plasma and seeded in either 5-well canonical plates (Corning, for flow cytometry analysis) or 8-well microslides (ibidi, for time-lapse microscopy). Plates were incubated for 4 or 18 h at 37°C + 5% CO_2.

Cell death analysis by flow cytometry

If indicated, pan-caspase inhibitor Q-VD-Oph (50 μM; Sigma-Aldrich, St. Louis, MO, USA), caspase-1 inhibitor Z-YVAD-FMK (50 μM; Sigma-Aldrich), caspase-8 inhibitor Z-IETD-FMK (50 μM; R&D System, Minneapolis, MN, USA), MLKL inhibitor necrosulphonamide (NSA) (5 μM; Sigma-Aldrich), recombinant human sFasL (100 ng mL^{-1}; Enzo Life Sciences, Lausen, CH), Ultra-LEAF™ purified anti-human CD95 (FAS) blocking antibody (10 μg mL^{-1}, clone A16086F; Biolegend, San Diego, CA, USA), anti-human TNFRI (CD120a) antibody (2 μg mL^{-1}, 55R-170; Thermo Fisher), Ultra-LEAF™ purified anti-human TNFRII (CD120b) blocking antibody (2 μg mL^{-1}, clone 3G7A02; Biolegend) or respective DMSO and H_2O control were added prior to incubation. To induce apoptosis[36] or necroptosis,[37] neutrophils were treated with 30 ng mL^{-1} TNF-α (Biolegend) or simultaneously with 30 ng mL^{-1} TNF-α (Biolegend), 250 nM SMAC mimetics (birinapant; Selleckchem, Houston, TX, USA) and 10 μM IDN-6556 (Sigma-Aldrich) for 4 h. After the incubation period, plates were centrifuged at 500 *g* (full acceleration and brakes) for 6 min. Supernatants were collected for further analyses, and the wells were washed once with FACS buffer (DPBS + 5% foetal calf serum and 1 mM EDTA). Cells were stained with anti-CD66b APC (G10F5) from Thermo Fisher in FACS buffer for 30 min at 4°C. The wells were washed once with Annexin V buffer (Biolegend), and cells were stained with Annexin V-FITC and 7AAD (Biolegend) for 30 min at RT. The plates were acquired on an Attune NxT. The gating strategy is depicted in Supplementary figure 1.

Lactate dehydrogenase release measurement

Supernatants were incubated 1:2 with the substrate solution of the CytoTox 96® Non-Radioactive Cytotoxicity Assay (Promega, Dübendorf, CH) for 30 min in the dark in a 96-well plate (Greiner, Kremsmünster, AUT), after which the stop solution was added. The resulting absorbance of the converted substrate due to released lactate dehydrogenase (LDH) was measured at 490 nm.

DNA-release measurement

Supernatants were incubated 1:2 with 60 nM SYTOX™ Green (Thermo Fisher) for 30 min at 4°C in a 96-well black-bottom plate (Greiner). The fluorescence of the bound DNA was measured in a fluorescence plate reader (Molecular Probes, Eugene, OR, USA) with excitation at 488 nm and emission at 520 nm.

Cell surface receptors and ligand analysis by flow cytometry

To assess intracellular FasL levels, GolgiStop™ (BD Biosciences, Franklin Lakes NJ, USA) was added according to the manufacturer's instruction for 4 h. After the incubation period, plates were centrifuged and washed once with DPBS. Cells were stained with the Fixable LIVE/DEAD™ Near-IR Dead Cell Marker (Thermo Fisher) in DPBS for 25 min at 4°C. Next, the wells were washed once with FACS buffer and cells were stained with anti-CD66b APC or PE-Cy7 (G10F5) and anti-IFNAR-1 PE (MAR1-5A3) from Thermo Fisher, and anti-Fas BV421 (DX2), anti-TRAIL-R1 APC (DJR1) and anti-TNFRI PE (W15099A) all from Biolegend in FACS buffer for 30 min at 4°C. For intracellular staining, the cells were fixed for 15 min at 4°C in the Fix/Perm Solution A from Fix/Perm Kit. Next, staining with anti-FasL BV421 (NOK-1) from Biolegend or anti-RIPK1 AF488 (Polyclonal) from Bioss Antibodies (Woburn MA, USA) was carried out in Fix/Perm solution B for 30 min at 4°C. The plates were acquired on an Attune NxT.

Time-lapse microscopy

After adding the cells to the microslides, 150 nM SYTOX™ Green (Thermo Fisher) and 2 μM Hoechst 33342 (Thermo Fisher) were added and the slides were centrifuged at 500 *g* (low acceleration and brakes) for 3 min. Microslides were imaged for 4 h at 37°C on a fully automated Olympus IX83 microscope (Olympus Life Science, Shinjuku, JP) with a 40× objective (UPLFLN40XPH-2), illuminated with a PE-4000 LED System through a quad-band filter set (U-IFCBL50). Eight observation positions per well (condition) were assigned before the time-lapse was started to avoid potential observer bias. Images were taken every 10 min. The proportion of dead neutrophils was assessed as described in Supplementary figure 2a: after filtering the nuclei on the Hoechst signal and watershed segmentation, cells were tracked through time and either assigned the category 'live' or 'dead' based on the value of the SYTOX Green signal. Assigned dead cells were counted until the end of the experiment, even after the disappearance of the fluorescent signal. The exponential death rate was fitted from the first few hours of the experiment. Images were processed using the ImageJ software.

Histology

Formalin-fixed paraffin-embedded tissue sections were pre-treated with the BOND Epitope Retrieval Solution 2 (Leica Biosystems, Wetzlar, GER) at 100°C for 30 min. They were stained with RIPK1 (ab72139, clone 7H10, dilution 1:1500), RIPK3 (ab62344, polyclonal, dilution 1:100) and MLKL (ab184718, EPR17514, dilution 1:100), all from Abcam; pMLKL (mab91871, clone 954724, dilution 1:200) from Novus Biologicals; and mouse IgG2b kappa isotype control (eBMG2b), mouse IgG2a isotype control and rabbit IgG isotype control all from Thermo Fisher, for 30 min. For detection, the slides were stained with the Bond Polymer Refine Detection HRP Kit (Leica Biosystem), according to the manufacturer's instruction, and counterstained with haematoxylin. For background information of the obtained biopsies, see Supplementary table 3.

Statistical analyses

The number of donors can be found in the corresponding figure legends. Samples were assessed for normal distribution. Differences between the two groups were calculated using either the unpaired *t*-test, Mann–Whitney *U*-test, paired *t*-test or Wilcoxon signed-rank test in Prism (GraphPad, San Diego CA, USA). The correlation of clinical parameters was computed using the non-parametric Spearman correlation in Prism.

ACKNOWLEDGMENTS

We thank our patients for participating in this study. Furthermore, we thank Andre Fitsche, Christiane Mittmann and Susanne Dettwiler for their help with histology. This work was funded by the SNSF Project Grant 31003A_176252 (to ASZ), the SNF Biobanking Grant 31BK30_185401 (to ASZ), the Uniscientia Foundation Grant (to ASZ and SMS), the Swedish Society for Medical Research (SSMF) Foundation Grant P17-0179 (to SMS), the Promedica Foundation 1449/M (to SDB) and unrestricted funds (to RAS).

CONFLICT OF INTEREST

The authors declare no conflict of interest.

AUTHOR CONTRIBUTIONS

Tiziano Angelo Schweizer: Conceptualization; Data curation; Formal analysis; Investigation; Methodology; Validation; Visualization; Writing-original draft; Writing-review & editing. **Srikanth Mairpady Shambat:** Conceptualization; Formal analysis; Investigation; Methodology; Validation; Writing-original draft; Writing-review & editing. **Clément Vulin:** Data curation; Formal analysis; Investigation; Software; Visualization; Writing-review & editing. **Sylvia Hoeller:** Investigation; Visualization; Writing-review & editing. **Claudio Tirso Acevedo:** Investigation; Validation; Writing-review & editing. **Markus Huemer:** Investigation; Writing-review & editing. **Alejandro Gomez-Mejia:** Investigation; Writing-review & editing. **Chun-Chi Chang:** Investigation; Writing-review & editing. **Jeruscha Baum:** Investigation; Writing-review & editing. **Sanne Hertegonne:** Investigation; Writing-review & editing. **Eva Hitz:** Investigation; Writing-review

& editing. **Thomas Scheier:** Investigation; Validation; Writing-review & editing. **Daniel Andrea Hofmaenner:** Investigation; Writing-review & editing. **Philipp Karl Buehler:** Investigation; Writing-review & editing. **Holger Moch:** Resources; Supervision; Writing-review & editing. **Reto Schuepbach:** Resources; Supervision; Writing-review & editing. **Silvio Daniel Brugger:** Funding acquisition; Project administration; Supervision; Validation; Writing-review & editing. **Annelies Sophie Zinkernagel:** Conceptualization; Funding acquisition; Project administration; Resources; Supervision; Validation; Writing-review & editing.

REFERENCES

1. Huang C, Wang Y, Li X *et al*. Clinical features of patients infected with 2019 novel coronavirus in Wuhan, China. *Lancet* 2020; **395**: 497–506.
2. Metzemaekers M, Cambier S, Blanter M *et al*. Kinetics of peripheral blood neutrophils in severe coronavirus disease 2019. *Clin Transl Immunol* 2021; **10**: 1–18.
3. Middleton EA, He X, Denorme F *et al*. Neutrophil extracellular traps contribute to immunothrombosis in COVID-19 acute respiratory distress syndrome. *Blood* 2020; **136**: 1169–1179.
4. Radermecker C, Detrembleur N, Guoit J *et al*. Neutrophil extracellular traps infiltrate the lung airway, interstitial and vascular compartments in severe Covid-19. *J Exp Med* 2020; **217**: e20201012s.
5. Nakazawa D, Desai J, Steiger S *et al*. Activated platelets induce MLKL-driven neutrophil necroptosis and release of neutrophil extracellular traps in venous thrombosis. *Cell Death Discov* 2018; **4**: 71.
6. Feoktistova M, Geserick P, Kellert B *et al*. CIAPs block ripoptosome formation, a RIP1/caspase-8 containing intracellular cell death complex differentially regulated by cFLIP isoforms. *Mol Cell* 2011; **43**: 449–463.
7. Schilling R, Geserick P, Leverkus M. Characterization of the ripoptosome and its components: implications for anti-inflammatory and cancer therapy. *Methods Enzymol* 2014; **545**: 83–102.
8. Cook WD, Moujalled DM, Ralph TJ *et al*. RIPK1- and RIPK3-induced cell death mode is determined by target availability. *Cell Death Differ* 2014; **21**: 1600–1612.
9. Tummers B, Mari L, Guy CS *et al*. Caspase-8-dependent inflammatory responses are controlled by its adaptor, FADD, and necroptosis. *Immunity* 2020; **52**: 1–13.
10. Van Der Linden M, Westerlaken GHA, Van Der Vlist M, Van Montfrans J, Meyaard L. Differential signalling and kinetics of neutrophil extracellular trap release revealed by quantitative live imaging. *Sci Rep* 2017; **7**: 1–11.
11. Corriden R, Hollands A, Olson J *et al*. Tamoxifen augments the innate immune function of neutrophils through modulation of intracellular ceramide. *Nat Commun* 2015; **6**: 8369.
12. Mairpady Shambat S, Gomez-Mejia A, Schweizer TA *et al*. Neutrophil and monocyte dysfunctional effector response towards bacterial challenge in critically-ill COVID-19 patients. *bioRxiv* 2020. doi:https://doi.org/10.1101/2020.12.01.406306
13. Qin C, Zhou L, Hu Z *et al*. Dysregulation of immune response in patients with coronavirus 2019 (COVID-19) in Wuhan, China. *Clin Infect Dis* 2020; **71**: 762–768.
14. Hazard D, Kaier K, Von Cube M *et al*. Joint analysis of duration of ventilation, length of intensive care, and mortality of COVID-19 patients: A multistate approach. *BMC Med Res Methodol* 2020; **20**: 1–9.
15. Horby P, Wei Shen L, Emberson JR *et al*. Dexamethasone in hospitalized patients with Covid-19. *N Engl J Med* 2021; **384**: 693–704.
16. Mocarski ES, Upton JW, Kaiser WJ. Viral infection and the evolution of caspase 8-regulated apoptotic and necrotic death pathways. *Nat Rev Immunol* 2012; **12**: 79–88.
17. Duan X, Liu X, Liu N *et al*. Inhibition of keratinocyte necroptosis mediated by RIPK1/RIPK3/MLKL provides a protective effect against psoriatic inflammation. *Cell Death Dis* 2020; **11**: 134.
18. Silvin A, Chapuis N, Dunsmore G *et al*. Elevated calprotectin and abnormal myeloid cell subsets discriminate severe from Mild COVID-19. *Cell* 2020; **182**: 1401–1418.e18.
19. Varga Z, Flammer AJ, Steiger P *et al*. Endothelial cell infection and endotheliitis in COVID-19. *Lancet* 2020; **395**: 1417–1418.
20. Wang X, He Z, Liu H, Yousefi S, Simon H-U. Neutrophil necroptosis is triggered by ligation of adhesion molecules following GM-CSF priming. *J Immunol* 2016; **197**: 4090–4100.
21. Wicki S, Gurzeler U, Wei-Lynn Wong W, Jost PJ, Bachmann D, Kaufmann T. Loss of XIAP facilitates switch to TNFα-induced necroptosis in mouse neutrophils. *Cell Death Dis* 2016; **7**: e2422.
22. Abers MS, Delmonte OM, Ricotta EE *et al*. An immune-based biomarker signature is associated with mortality in COVID-19 patients. *JCI Insight* 2021; **6**: e144455.
23. O'Reilly LA, Tai L, Lee L *et al*. Membrane-bound Fas ligand only is essential for Fas-induced apoptosis. *Nature* 2009; **461**: 659–663.
24. O'Donnell JA, Kennedy CL, Pellegrini M *et al*. Fas regulates neutrophil lifespan during viral and bacterial infection. *J Leukoc Biol* 2015; **97**: 321–326.
25. Schenk RL, Gangoda L, Lawlor KE, O'Reilly LA, Strasser A, Herold MJ. The pro-survival Bcl-2 family member A1 delays spontaneous and FAS ligand-induced apoptosis of activated neutrophils. *Cell Death Dis* 2020; **11**: 474.
26. Margaryan S, Witkowicz A, Arakelyan A, Partyka A, Karabon L, Manukyan G. sFasL-mediated induction of neutrophil activation in patients with type 2 diabetes mellitus. *PLoS One* 2018; **13**: e0201087.
27. Bellesi S, Metafuni E, Hohaus S *et al*. Increased CD95 (Fas) and PD-1 expression in peripheral blood T lymphocytes in COVID-19 patients. *Br J Haematol* 2020; **95**: 1–5.
28. Fielding CA, McLoughlin RM, McLeod L *et al*. IL-6 regulates neutrophil trafficking during acute inflammation via STAT3. *J Immunol* 2008; **181**: 2189–2195.
29. Maeda K, Malykhin A, Teague-Weber BN, Sun XH, Farris AD, Coggeshall KM. Interleukin-6 aborts lymphopoiesis and elevates production of myeloid cells in systemic lupus erythematosus-prone B6.Sle1.Yaa animals. *Blood* 2009; **113**: 4534–4540.
30. Liu Z, Li J, Long W *et al*. Bilirubin levels as potential indicators of disease severity in coronavirus disease patients: a retrospective cohort study. *Front Med* 2020; **7**: 598870.

31. Yamada Y, Endo S, Nakae H *et al*. Examination of soluble Fas (sFas) and soluble Fas ligand (sFasL) in patients with burns. *Burns* 2003; **29**: 799–802.
32. Luo J, Wang Y, Yu B, Qian H, He Y, Shi G. A potential of sFasL in preventing gland injury in Sjogren's syndrome. *Biomed Res Int* 2017; **2017**: 5981432.
33. Ronchetti S, Ricci E, Migliorati G, Gentili M, Riccardi C. How glucocorticoids affect the neutrophil life. *Int J Mol Sci* 2018; **19**: 4090.
34. Yang JW, Yang L, Luo RG, Xu JF. Corticosteroid administration for viral pneumonia: COVID-19 and beyond. *Clin Microbiol Infect* 2020; **26**: 1171–1177.
35. Buehler PK, Zinkernagel AS, Hofmaenner DA *et al*. Bacterial pulmonary superinfections are associated with unfavourable outcomes in critically ill COVID-19 patients. *Cell Reports Med* 2021; **2**: 100229.
36. Salamone G, Giordano M, Trevani AS *et al*. Promotion of neutrophil apoptosis by TNF-α. *J Immunol* 2001; **166**: 3476–3483.
37. Tanzer MC, Frauenstein A, Stafford CA, Phulphagar K, Mann M, Meissner F. Quantitative and dynamic catalogs of Proteins released during apoptotic and necroptotic cell death. *Cell Rep* 2020; **30**: 1260–1270.e5.

Supporting Information

Additional supporting information may be found online in the Supporting Information section at the end of the article.